INSTITUTE OF PHYSICS PUBLISHING MEASUREMENT SCIENCE AND TECHNOLOGY

Meas. Sci. Technol. **15** (2004) 1716–1721 PII: S0957-0233(04)80573-3

A study on the digital nano-moiré method and its phase shifting technique

Huimin Xie[1], Zhanwei Liu[1], Daining Fang[1], Fulong Dai[1], Hongjun Gao[2] and Yapu Zhao[3]

[1] Department of Engineering Mechanics, FML, Tsinghua University, 100084 Beijing, People's Republic of China
[2] Opening Laboratory of Vacuum Physics, Chinese Academy of Science, 100080 Beijing, People's Republic of China
[3] LNM, Institute of Mechanics, Chinese Academy of Science, 100080 Beijing, People's Republic of China

E-mail: liuzw01@mails.tsinghua.edu.cn

Received 19 June 2003, in final form 30 April 2004
Published 23 July 2004
Online at stacks.iop.org/MST/15/1716
doi:10.1088/0957-0233/15/9/007

Abstract
A novel digital nano-moiré method is proposed to measure the in-plane nanoscopic deformation of an object. In the measurement, the periodic lattice of a single-crystal material acts as a specimen grating while a digital reference grating (DRG) is prepared by computer software. These two gratings overlap to generate a moiré fringe pattern. The preparation of the grating, the formation principle of digital nano-moiré fringes and its relative phase shifting technique are described in detail. A typical experiment was conducted with a highly oriented pyrolytic graphite (HOPG) sample. The residual deformation of the irradiated HOPG sample was measured using this method. The experiment result verifies the feasibility of this method, and demonstrates the potential for further applications.

Keywords: digital grating, nano-moiré method, phase-shifting technique, crystal lattice

1. Introduction

The moiré method was introduced by Weller [1] in 1948 and has been improved by many researchers. The classical moiré method, referred to as geometric or coarse moiré, has been widely used in experimental stress analysis [2–7]. However, because the gratings utilized in the geometric moiré method have a frequency lower than 100 lines mm^{-1}, this method can only be applied to measure large deformation.

Moiré interferometry developed by Post [8] is a full-field deformation measurement method. It offers a unique combination of high sensitivity, excellent contrast, wide range and high spatial resolution. Since the 1980s this method has been widely used for the deformation measurement at both macro- and meso-scales. According to the principle of moiré interferometry, the applicable grating for moiré interferometry is confined in a range of frequency from 600 lines mm^{-1} to 2400 lines mm^{-1} with a visible laser. Thus, this method is limited to deformation measurement in a range over the submicron level.

In 1993, the electron beam moiré method was developed by Dally and Read [9]. In their work, electron beam lithography was used to produce gratings with very fine lines on the surface of a sample. These gratings can be used to measure micro-deformation with the moiré methods under high resolution microscopes. In a later report, a grating with a frequency of 10 000 lines mm^{-1} was successfully produced by electron beam lithography [10]. In 1993, Read *et al* [11] proposed the scanning moiré method. In their study, scanning lines in a SEM monitor or CCD video camera were used as a reference grating to form scanning moiré fringes. This method could provide an easy and effective way to improve the resolution in moiré measurement.

Asundi *et al* [12–14] proposed a logical moiré method and showed that it could measure in-plane deformation. They used two 1-bit binary digital gratings and the logical operators

(AND, OR, XOR) to generate moiré fringes. Kato *et al* [15] and Womack [16] proposed a real-time and quantitative fringe analyser based on a phase-shifting electronic moiré-pattern technique. Their work used a sinusoidal reference fringe pattern generated by a computer.

Recently, with the development of nanotechnology, various microscopy techniques have been widely used for processing, manufacture and measurement at the nanoscale [17, 18]. Manufacturing techniques to produce machinery, transducers and actuators of nanometre scale are being developed. Similar to ordinary structure at the macroscale, a nano-component will also deform under an external load. When the load exceeds the allowable limit, the structure will experience damage. The constitutive relation of materials and the mechanism of mechanical failure of a structure at the nanometre scale is becoming an interesting problem for researchers in mechanics and materials science. Solving the problem requires experimental techniques with nanometre sensitivity and spatial resolution. The above-mentioned methods cannot meet such requirements.

Hashimoto and Ueda [19] and Pashley [20] observed dislocation by means of a moiré pattern on electron micrographs in 1957. In their works, a crystal lattice was first introduced to serve as the specimen grating. In 1999, Dai and Xing [21] proposed a nano-moiré method in which a HREM (high resolution electron microscopy) image of crystal lattices acting as a specimen grating is superposed onto a unidirectional geometric grating as a reference one. Xie *et al* [22] developed a new scanning moiré method in which moiré patterns are formed by scanning lines of the CRT (cathode-ray tube) in an AFM system and the atomic lattice of mica.

In this paper, a novel digital nano-moiré method with atom-size sensitivity and spatial resolution is presented. Moiré fringes are generated by superposition of a digital reference grating on a crystal lattice. The method is successfully used to measure the deformation of HOPG. Some useful results are obtained.

2. Measurement principle of digital nano-moiré

2.1. Preparation for specimen grating and reference grating

A single crystal has a periodic lattice structure, which can consist of atoms, molecules or ions. The lattice can be considered as a specimen grating. Under a high resolution microscope, the lattice configuration can be observed at a suitable magnification and the image of this lattice can be recorded and digitized. In order to form a moiré pattern, a reference grating should be prepared. In this study, a sinusoidal digital grating is prepared using Matlab software. In order to make the moiré measurement, the reference grating and the specimen grating should have similar frequencies. A schematic diagram of specimen grating is shown in figure 1. Suppose the spatial frequency of a specimen grating in the y-axis direction is f_s, and the corresponding pitch is p_s. The pitch of the DRG is p_m.

In the experiment, a piece of HOPG with area of 3 mm × 3 mm × 1 mm is selected as a measured object. A lattice image of HOPG is captured by a scanning tunnelling microscope (STM) and shown in figure 2. The periodic structure of

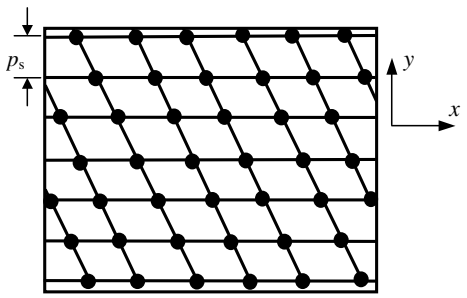

Figure 1. Schematic diagram of a crystal lattice.

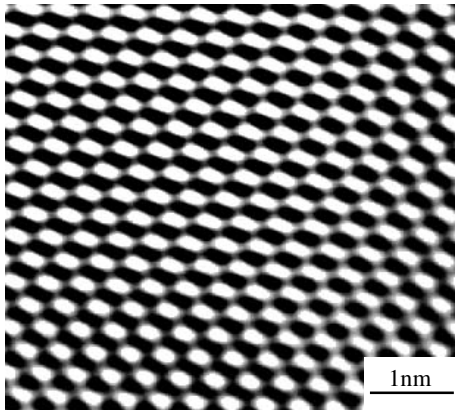

Figure 2. Periodic crystal lattice of HOPG.

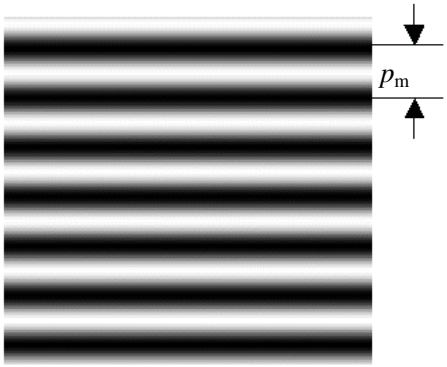

Figure 3. Sinusoidal digital grating (reference grating).

the crystal lattice (with a period of 0.246 nm) represents a grating with a frequency of 4065 041 lines mm^{-1}. Such a high-frequency grating allows the moiré measurement to reach atomic level sensitivity.

The recorded HOPG lattice images are converted into greyscale maps. The pitch of the specimen grating p_s before deformation is measured, which can be expressed as the pixel value. The maximum and minimum greyscale values and the sizes of the specimen grating in the x and y directions are also evaluated and defined as Q_1, Q_2, S_x and S_y, respectively. A digital grating is generated using Matlab6.0 according to these parameters. The digital grating can be expressed as a sinusoidal function:

$$M(y,x) = M_0 + M_1 \sin[w_1(y+\phi_1) + w_2(x+\phi_2)] \quad (x = 1, 2, 3, \ldots, S_x;\ y = 1, 2, 3, \ldots, S_y) \tag{1}$$

$$M_0 = (Q_1 + Q_2)/2 \qquad M_1 = (Q_1 - Q_2)/2$$

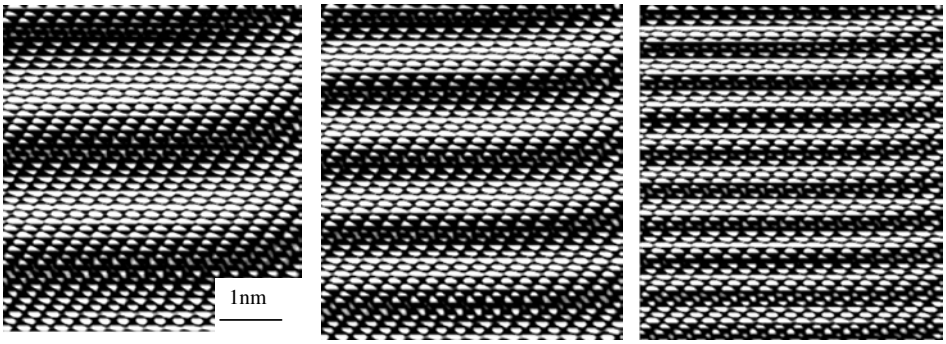

(*a*) (*b*) (*c*)

Figure 4. Digital parallel nano-moiré patterns with different reference gratings and the same specimen grating (its size is 5 nm × 5 nm, $p_s = 18$ pixel). (*a*) $p_m = 15.7$ pixel, (*b*) $p_m = 14.5$ pixel, (*c*) $p_m = 12.1$ pixel.

where M_0 acts as the background intensity (greyscale), w_1, w_2, ϕ_1 and ϕ_2 are the frequency and the original phase of the digital grating in the y and x directions, respectively; and $\arctan(w_2/w_1)$ is the angle between the grating line and the x direction. In the computer monitor, a digital grating is a rectangular grid of size $S_y \times S_x$. If a digital grating is composed of lines parallel to x-axis, the equation (1) can be simplified as

$$M(y, x) = M_0 + M_1 \sin[w_1(y + \phi_1)] \quad (y = 1, 2, 3, \ldots, S_y) \tag{2}$$

where $w_1 = 2\pi/p_m$, p_m is the pitch of the digital grating. In general, p_m is approximately equal to p_s. From equation (2), it can be seen that the function $M(y, x)$ has no relation with the parameter x. Figure 3 shows a configuration of the sinusoidal digital grating (reference grating).

2.2. The measurement principle of digital nano-moiré fringes

2.2.1. Digital parallel nano-moiré method. The specimen gratings are recorded before and after loading. Then they are independently superposed with the same DRG to form moiré fringes. By subtracting the specimen grating and the DRG as in [12], two moiré patterns can be obtained. One is known as the initial moiré pattern (also called carrier moiré), which reflects the initially mismatched interference between the two gratings. In general, the moiré fringes can be parallel or angular ones, which can be formed by adjusting the direction of the specimen grating or the reference grating. The other is called the deformation moiré pattern with carrier. When the initial moiré fringes are parallel, the moiré pattern can be called digital parallel nano-moiré. In the measurement, the reference grating lines are mainly aligned in the y direction. Moiré fringes are generated and can reflect deformation in the y-axis.

From the initial moiré pattern, the initial virtual displacement v_y^0 and strain ε_y^0 in the y direction can be measured as

$$v_y^0 = X p_s / N \tag{3}$$

$$\varepsilon_y^0 = \frac{\partial v_y^0}{\partial y} = \pm \frac{p_s/N}{s_0/N} = \pm \frac{p_s}{s_0} \tag{4}$$

where X is the fringe order, s_0 is the spacing between two adjacent fringes and N is the magnification of the microscope used.

After exerting a load, the deformation moiré pattern with carrier is generated. This moiré pattern includes information on the distortion of the specimen in the y direction. Using this moiré pattern, the displacement v_y^1 and normal strain component in the y direction ε_y^1 are calculated. The equations can be expressed as

$$v_y^1 = X' p_s / N \tag{5}$$

$$\varepsilon_y^1 = \frac{\partial v_y^1}{\partial y} = \pm \frac{p_s/N}{s_1/N} = \pm \frac{p_s}{s_1} \tag{6}$$

where X' is the fringe order and s_1 is the spacing between two adjacent fringes corresponding to the deformation moiré patterns with carrier.

Subtracting equations (3) from (5) and (4) from (6), the real displacement and normal strain incurred by the load in the y direction can be calculated as

$$v_y = v_y^1 - v_y^0 = (X' - X) p_s / N \tag{7}$$

$$\varepsilon_y = \varepsilon_y^1 - \varepsilon_y^0 = \pm \frac{p_s}{s_1} - \left(\pm \frac{p_s}{s_0} \right). \tag{8}$$

The sign of the normal strain can be determined by rotating the specimen grating. When the fringes move in the same direction as this rotation, the normal strain is compressive. Otherwise, the normal strain is tensile. The sign of the normal strain can also be determined by the state of tension or compression, if the loading situation of the specimen is clear.

In this paper, digital parallel nano-moiré patterns are generated with different grating parameters, and shown in figures 4 and 5. Figure 4 shows the mismatched moiré patterns created with different reference grating (pitches p_m is varied) and the same specimen grating. It can be seen from these figures that moiré fringes and atomic lattices coexist. Figure 5 shows the moiré patterns with different specimen and reference gratings (grating pitches are different). Figure 5(*c*) is the moiré pattern formed by scanning lines of a computer monitor (the pitch p_m is 1 pixel) and the specimen grating.

2.2.2. Digital angular nano-moiré method. When the digital reference grating is rotated by a small angle with respect to the specimen grating, an angular nano-moiré fringe can be obtained. Figure 6 is a schematic diagram of geometric relationship between angular moiré fringes and adjacent grating lines. Two parallel lines AB and OC are two adjacent

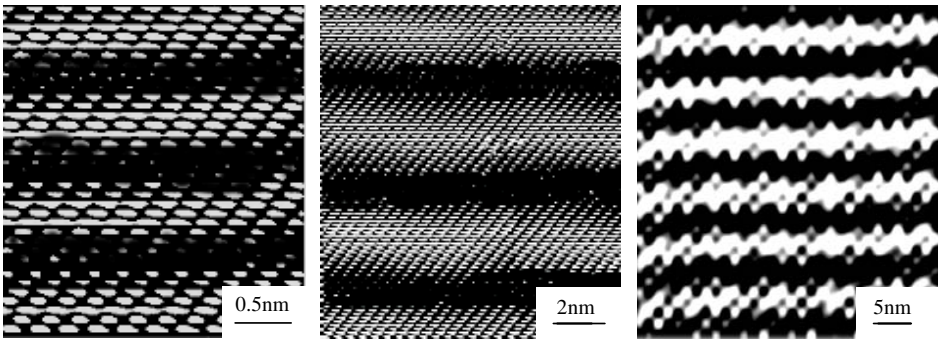

Figure 5. Digital parallel nano-moiré patterns with different specimen and reference gratings. (*a*) $p_m = 36$ pixel, (*b*) $p_m = 7$ pixel, (*c*) $p_m = 1$ pixel.

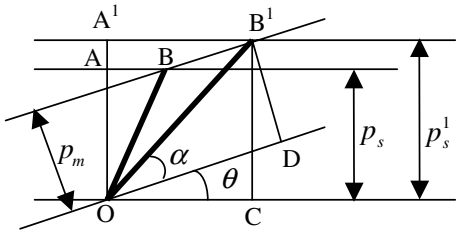

Figure 6. Geometric relationship between moiré fringes and adjacent grating lines.

lines of the specimen grating before deformation; p_s^1 is the pitch of the specimen grating after deformation; BB^1 and OD are two adjacent lines of the reference grating; OB and OB^1 are the centre lines of bright stripes of moiré fringes before and after deformation, respectively; α is the angle between the reference grating and moiré fringe; θ is the angle between the reference grating and the specimen grating.

From figure 6, the normal strain in the y direction can be directly calculated:

$$\varepsilon_y = \frac{BB^1}{OB} = \frac{OB^1 - OB}{OB} = \frac{p_s^1 - p_s}{p_s}. \tag{9}$$

According to the geometrical relation between the triangles OB^1D and OB^1C, equation (9) can be further expressed as

$$\varepsilon_y = \frac{p_m}{p_s} \times \frac{\sin(\alpha + \theta)}{\sin\alpha} - 1. \tag{10}$$

In the angular moiré measurement, as in the parallel nano-moiré method, moiré fringes were generated before and after deformation of the specimen. The strain component (before loading) ε_y^0 and the strain component (after loading) ε_y^1 are calculated. The real normal strain caused by load is $\varepsilon_y = \varepsilon_y^1 - \varepsilon_y^0$, whose sign is determined by expression (10). Digital angular nano-moiré patterns with different θ are shown in figure 7.

3. Principle of the phase-shifting technique for the digital nano-moiré method

The phase-shifting algorithms for the digital moiré method can still be used [13]. The light intensity (greyscale) distributions of moiré fringe can be expressed as

$$I(x, y) = I_0(x, y)\{1 + b(x, y)\cos[\phi(x, y) + \delta_i]\} \tag{11}$$

where $I_0(x, y)$ is the intensity of the background, $b(x, y)$ is a contribution of alternating light intensity, $\phi(x, y)$ is a function of fringe phase and δ_i is the amount of phase shifting. If $\delta_i = 0, \pi/2, \pi, 3\pi/2$, respectively, we can obtain

$$I_1(x, y) = I_0(x, y)\{1 + b(x, y)\cos[\phi(x, y)]\} \tag{12}$$

$$I_2(x, y) = I_0(x, y)\{1 + b(x, y)\cos[\phi(x, y) + \pi/2]\} \tag{13}$$

$$I_3(x, y) = I_0(x, y)\{1 + b(x, y)\cos[\phi(x, y) + \pi]\} \tag{14}$$

$$I_4(x, y) = I_0(x, y)\{1 + b(x, y)\cos[\phi(x, y) + 3\pi/2]\} \tag{15}$$

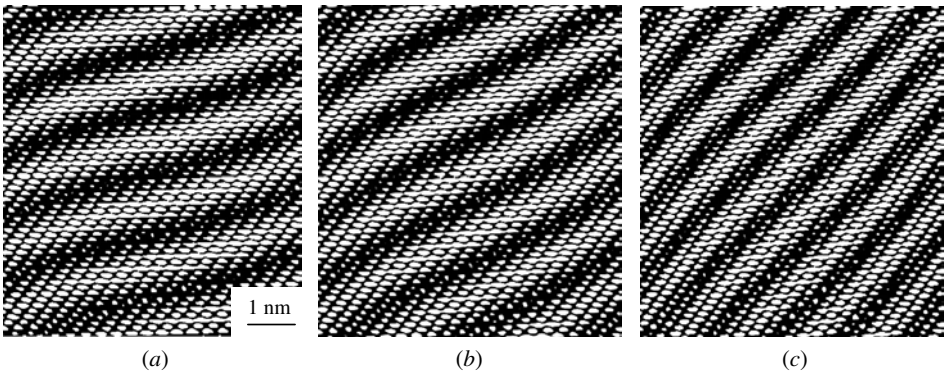

Figure 7. Digital angular nano-moiré patterns with different θ ($p_s = p_m = 16$ pixel). (*a*) $\theta = 2^\circ$, (*b*) $\theta = 4^\circ$, (*c*) $\theta = 8^\circ$.

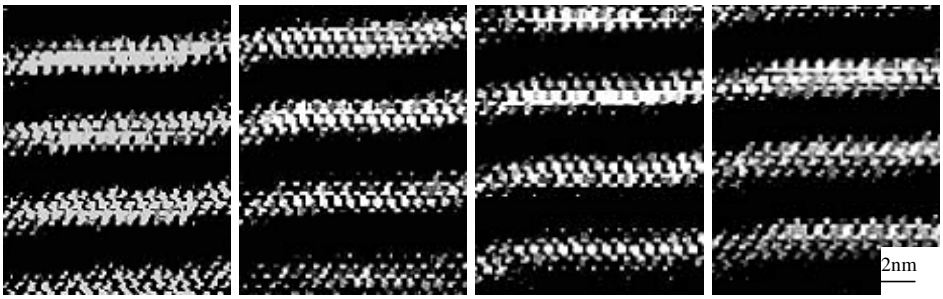

Figure 8. Four steps of phase-shifting moiré patterns. (*a*) $\delta = 0$, (*b*) $\delta = \pi/2$, (*c*) $\delta = \pi$, (*d*) $\delta = 3\pi/2$.

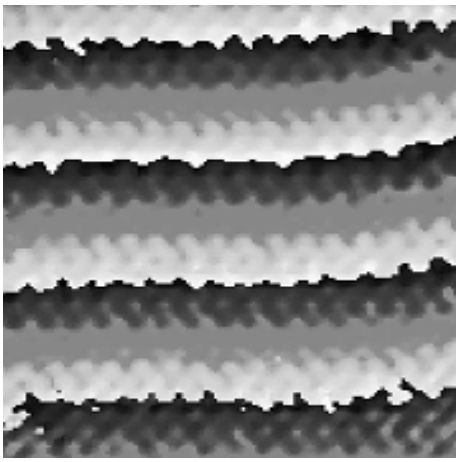

Figure 9. Wrapped phase of digital moiré patterns.

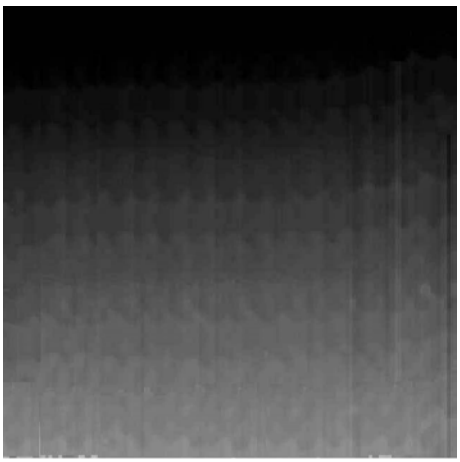

Figure 10. Unwrapped phase of digital moiré patterns.

From equations (12)–(15), the phase distribution can be written as

$$\phi(x, y) = \arctan\frac{I_4 - I_2}{I_1 - I_3}. \tag{16}$$

When the digital reference grating moves in the *y* direction by four steps of 0, $\frac{1}{4}p_{\mathrm{m}}$, $\frac{1}{2}p_{\mathrm{m}}$, $\frac{3}{4}p_{\mathrm{m}}$, accordingly, the phase of moiré patterns shifts by 0, $\frac{1}{2}\pi$, π, $\frac{3}{2}\pi$, respectively. As an example, the phase-shifting technique is applied to process parallel digital nano-moiré. The four steps of phase-shifting moiré patterns are shown in figure 8.

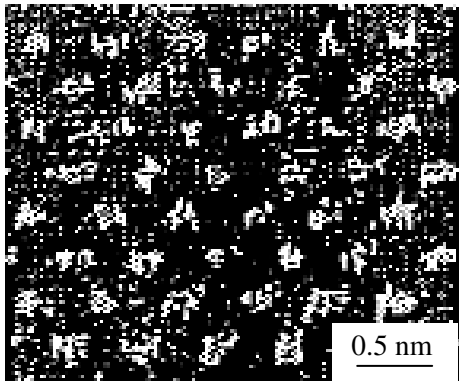

Figure 11. The crystal lattice structure of the illuminated HOPG ($d_0 = 0.01$ mm).

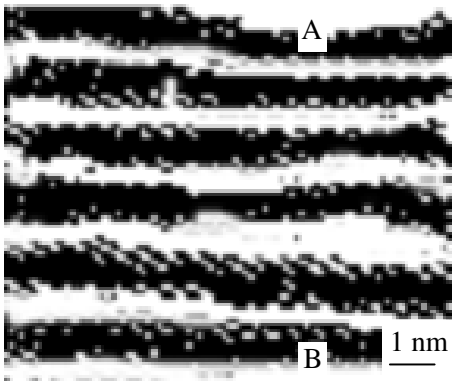

Figure 12. Digital moiré pattern in the *y* direction.

A filtering technique can be used to improve the fringe contrast. The four moiré patterns were processed to reduce the noise using the filtering function in Matlab. After this process, a wrapped phase image is obtained according to equation (16) and is shown in figure 9. After eliminating the phase discontinuities according to the technique in [13], an unwrapped phase image is formed as in figure 10.

4. Application

The residual deformation of the irradiated single crystal HOPG was studied with this method. In the experiment, the surface of the HOPG sample was irradiated by a pulsed YAG laser. The laser energy was determined as 75 mJ, and its frequency was 50 Hz. The diameter of the illuminated laser facula was

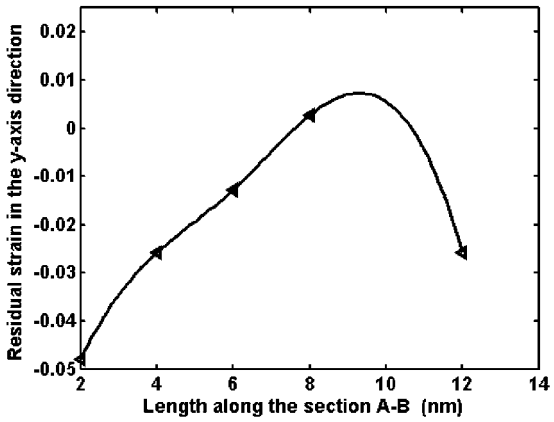

Figure 13. Residual strain distribution along section A–B in the *y* direction.

1 mm. The atomic structures (crystal lattice) of the irradiated HOPG are shown in figure 11, which refers to the atomic configurations at the positions of $d_0 = 0.01$ mm (d_0 is the distance between the facula centre and the measuring point). The digital moiré pattern formed using the above method in the *y* direction is shown in figure 12.

The residual deformations were calculated using the initial moiré pattern and the deformation moiré pattern with carrier, and the result is shown in figure 13.

5. Conclusions

(1) The digital nano-moiré method is proposed. The successful experimental results verified that this method is feasible. The displacement measurement sensitivity of this method can reach the pitch of the lattice of a single crystal (sub-nanometre level), which depends on the material used.
(2) The digital phase-shifting technique is developed in this study. Experimental results show that this technique is effective in the processing images of nano-moiré fringes.
(3) A sinusoidal digital grating has been designed, and it can be very conveniently used in the formation of angular moiré and the phase-shifting process. The critical pitch of a DRG is 1 pixel.
(4) When compared with the TEM nano-moiré method, this method can use a computer-generated grating as the DRG, and thus a substantial reference grating need not be prepared. The cost of the experiment is thus reduced, and the working efficiency could obviously be improved.

Acknowledgment

The work is supported by the National Natural Science Foundation of China (under grants 10232030, 10121202), the Key grant project of the Chinese Ministry of Education (no 0306), the Research Foundation from Tsinghua University, a visiting fund from the Opening Laboratory of Vacuum Physics, and LNM at the Chinese Academy of Science, and the Project sponsored by SRF for ROCS, SEM.

References

[1] Weller R and Shepard B M 1948 Displacement measurement by mechanical interferometry *Proc. Soc. for Exp. Stress Anal.* **6** 35–8
[2] Morse S A, Durelli J and Sciammarella C A 1960 Geometry of moiré fringes in strain analysis *J. Eng. Mech. Div., ASCE* **86** 105–26
[3] Sciammarela C A and Durelli A J 1961 Moiré fringes as a means of analyzing strains *J. Eng. Mech. Div., ASCE* **87** 55–74
[4] Durelli A J and Parks V J 1970 *Moiré Analysis of Strain* (Englewood Cliffs, NJ: Prentice Hall)
[5] Theocaris S 1969 *Moiré Fringe in Strain Analysis* (Oxford: Pergamon)
[6] Post D, Han B and Ifju P 1994 *High Sensitivity Moiré* (Berlin: Springer)
[7] Chiang F P 1982 Moiré method of strain analysis *Manual on Experimental Stress Analysis* 5th edn, ed J F Doyle and J W Phillips (Bethel, CT: Society for Experimental Mechanics) pp 107–35
[8] Post D 1988 Sharping and multiplication of moiré fringe *Exp. Mech.* **28** 329–35
[9] Dally J W and Read D T 1993 Electron-beam moiré *Exp. Mech.* **33** 270–7
[10] Kishimoto E M and Shinya N 1993 Micro-creep deformation measurement by a moiré method using electron beam lithography and electron beam scan *Opt. Eng.* **32** 522–6
[11] Read D T, Dally J W and Szanto M 1993 Scanning moiré at high magnification using optical methods *Exp. Mech.* **33** 110–6
[12] Asundi A and Yung K H 1991 Logical moiré and applications *Exp. Mech.* **31** 236–42
[13] Asundi A and Yung K H 1991 Phase shifting and logical moiré *J. Opt. Soc. Am.* A **18** 1591–600
[14] Asundi A and Wong C M 1991 Shadow moiré using LCD projection panel *Exp. Tech.* **15** 44–8
[15] Kato J, Yamaguhci I, Nakamura T and Kuwashima S 1997 Video-rate fringe analyzer based on phase shifting electronic moiré patterns *Appl. Opt.* **36** 8403–12
[16] Womack K H 1984 Interferometric phase measurement using spatial synchronous detection *Opt. Eng.* **23** 391–5
[17] Xie H M, Dai F L, Yang H, Liu N, Dietz P and Schmidt A 1998 The residual deformation measurement of nanometer crack in Si(111)7 × 7 with the scanning tunneling microscope *Scanning Probe Microsc.* **1** 181–5
[18] Chen C J 1993 *Introduction to Scanning Tunnel Microscope* (New York: Oxford University Press)
[19] Hashimoto H and Ueda R 1957 Detection of dislocation by the moiré pattern in electron micrographs *Acta Cryst.* **10** 143
[20] Pashley D W 1957 Observation of dislocation in metals by means of moiré pattern on electron micrographs *Nature* **179** 752–5
[21] Dai F L and Xing Y M 1999 Nano-moiré method *Acta Mech. Sin.* **15** 283–8
[22] Xie H M, Kishimoto S, Asundi A, Chai G B and Norio S Y 2000 In-plane deformation measurement using the atomic force microscope moiré method *Nanotechnology* **11** 24–9